IJES *Iranian Journal of Earth Sciences*
Vol. 13, No. 2, 2021, 77-93.

Seismic risk assessment for central Indo-Gangetic Plains, India

Manikya Choudari Raghucharan*[1], Surendra Nadh Somala [2], Olga Erteleva [3], Evgenii Rogozhin [3]

1. Indian Institute of Technology Hyderabad, Hyderabad - 502285, India
2. Department of Civil Engineering, Indian Institute of Technology Hyderabad, Hyderabad - 502285, India
3. Schmidt Institute of Physics of the Earth, Russian Academy of Sciences, Moscow – 123242, Russia

Received 11 February 2020; accepted 23 September 2020

Abstract

Seismic hazard for the central indo-gangetic plains (CIGP) is either available in terms of generalized hazard spectrum as per IS 1893:2016 or in terms of only Peak Ground Acceleration (PGA) at the city level. Also, the study region falls in the seismic gap region, which has a potential for an earthquake of Mw>8.0. Hence, in this study, the seismic risk is assessed for the first time at the district level in the seismically critical region of India, the CIGP. In addition, the relative contribution of parametric and model uncertainties is also quantified from sensitivity analysis. Seismic risk results reveal that mud mortar bricks with temporary roofing (MMB) have the highest collapse probability of ~0.6. Further, brick walls with stone roof (BSR) and brick walls with metal sheet roof (BMS) also have high extensive and collapse damage compared to other building groups. These building types need immediate retrofitting / replacement for effective disaster mitigation. Also, geo-unit Allahabad, even though lying in zone II as per IS 1893:2016, has the most number of homeless and uninhabitable dwellings. Further, for a future earthquake of magnitude in the range of M_w 7.5 and 8.5, the expected financial loss might vary from 60 to 150 billion dollars, and the human loss might vary between 0.8 and 2.8 lakhs, respectively. Finally, results from this study will create awareness in the general public, policymakers, and structural engineers for taking up necessary mitigation measures on the existing buildings of CIGP for better preparedness from a future strong earthquake.

Keywords: *Seismic hazard; Seismic risk; Central Indo-Gangetic Plains (CIGP); OpenQuake engine; SELENA*

1. Introduction

The seismic gap between the rupture zones of 1905 Kangra and 2015 Nepal earthquakes has the potential for producing an earthquake of magnitude > 8.0 (Bilham et al. 1995; Khattri 1999; Rajendran and Rajendran 2005; Bilham and Wallace 2005; Rajendran et al. 2015; Li et al. 2019). Further, the Indo-Gangetic plains (IGP), starting from Pakistan in the west and ending at Assam in the east, are one of the most populated basins in the world, covering 25 urban agglomerations with a population of more than a million (Bagchi and Raghukanth 2017). The principal cities like Delhi, Karachi, Dhaka, which lie in this region, have more than 15 million population.

The Indian part of IGP from Punjab to Assam has an urban population of more than 125 million, which is close to 1/3 of the total population of the nation (www.censusindia.gov.in), are under serious threat in the event of a great earthquake. In addition to the high population, the region is covered with sediments of thickness from 0.5 to 3.9 km, which not only amplify the seismic wave energy but also pose a threat to liquefaction (Chadha et al. 2016). Bilham (2009) has estimated casualties of around 0.3 million if an earthquake of Mw~8 occurs near an urban agglomeration of IGP. Seismic hazard levels for a given return period at a specific location were first computed by Cornell (1968), and a computer application for hazard estimation was developed by McGuire (1976).

---

*Corresponding author.
E-mail address (es): mcrc1055@gmail.com

The necessity of seismic hazard analysis has forced the development of numerous computer codes such as CRISIS, EQHAZ, EQRISK, EQRM, FRISK, National Seismic-Hazard Mapping Project (NSHMP), OpenSHA, SeisRisk, and OpenQuake Engine. These codes brought a handy contribution to the growth of seismic hazard assessment around the world. However, OpenQuake Engine, an open-source software that has reproducibility, testing, and community-based expansion capabilities, is selected for seismic hazard assessment in CIGP. Classical Probabilistic Seismic Hazard Analysis (PSHA) methodology is employed in this work for estimating seismic hazard levels for CIGP.

Seismic hazard assessment in the Indian sub-continent started way back in the 1970s by Basu and Nigam (1977), adopting a probabilistic approach to develop seismic hazard maps of PGA for a recurrence interval of 100 years. Khattri et al. (1984) prepared a PGA-based hazard map for a 10 % probability of exceedance in 50 years. Probabilistic seismic hazard maps developed by the Global Seismic Hazard Assessment Program (GSHAP) between 1992-1999 show contours of maximum PGA for 10 % probability of exceedance in 50 years' time window. Bhatia et al. (1999) conducted a probabilistic seismic hazard estimation for India under this framework. Parvez et al. (2003) attempted a deterministic hazard assessment of India.

Hazard estimations were also performed for smaller provinces or regions of India. Petersen et al. (2004) investigated seismicity models for Gujarat province

considering three fault sources in the north-western region. Sharma and Malik (2006) performed PSHA for north-east India. Jaiswal and Sinha (2007) reported a seismic hazard in Peninsular India, employing the probabilistic method. Mahajan et al. (2010) conducted PSHA for the north-western part of the Himalayan region. Kumar et al. (2013) conducted the seismic hazard analysis for the Lucknow region, taking into consideration local and active faults.

Working Committee Experts of National Disaster Management Authority headed by Prof. R. N. Iyengar along with several eminent professors from IITs, IMD, NGRI, SERC, GSI of India derived probabilistic hazard maps for India (NDMA 2011) by dividing entire India into thirty-two seismogenic zones. With the success of NDMA's effort for hazard estimation all over India, more studies have been undertaken by other researchers along similar lines (Nath and Thingbaijam 2012; Seetharam and Kolathayar 2013). The present zoning map given in the seismic code of India, IS 1893:2016, is prepared based on the earthquake catalogue up to 1993 and has not been updated till 2019. As per IS 1893, the design acceleration for the Design Basis Earthquake (DBE) is 0.18 g, and the Maximum Considered Earthquake (MCE) is 0.36 g for the service life of the structure, for the highest area, Zone V.

Keeping in view of several instances of severe to moderate shaking in the last century in Himalayan regions, the Indian code design acceleration for DBE is too optimistic and may underestimate the seismic loading in such a high seismicity region (Ghosh et al. 2012). Hence, a revised seismic hazard map for the country is essential considering new data, novel findings, and methodological advancements (Nath and Thingbaijam 2012). Das et al. (2006) recognized that one zone factor indicated in BIS (2002) for the whole of north-eastern India is unreliable, and Jaiswal and Sinha (2007) proclaimed that hazard in few regions of the Indian shield region is greater than BIS (2016); Mahajan et al. (2010) also came up with a similar conclusion for the north-western Himalayan region.

The region covered by the Himalayas and the Indo-Gangetic plains of India are especially susceptible due to higher levels of seismic hazard with the occurrence of four great earthquakes of magnitude > 8 (i.e., Assam 1950; Bihar–Nepal 1934; Kangra 1905 and Shillong 1897). The risk of Indian cities to seismic hazards has also elevated noticeably, demanding an appropriate hazard assessment, especially for urban centers with high population density in higher seismic zones (Verma and Bansal 2013). Hence, adopting site-specific seismic hazard for a region is appropriate than a generalized response spectrum given by IS 1893:2016, at least for areas under high seismic threat.

Seismic risk can be accredited as the risk of damage from an earthquake to a structure, system, and entity, which is often computed in terms of probability of damage, economic loss, and casualties in a region due to an occurrence of an earthquake. Seismic risk is often used synonymously with a more specific term called earthquake loss estimation (Lang 2013).

Initially, earthquake loss estimation studies were built on empirical information based on the macroseismic intensity scale due to the sparse instrumental ground motion records (McGuire 2004). Most of the intensity-based seismic loss estimation used data from the observed damage with expert opinion after an earthquake (Porter and Scawthron 2007).

With the invention of the nonlinear pushover analysis by Krawinkler and Seneviratna (1998) as well as the inception of the Capacity Spectrum Method (Freeman et al. 1975; Freeman 1978; ATC-40 1996), and the Displacement Coefficient Method (FEMA 273 1997; FEMA 356 2000; FEMA 440 2005), analytical approaches were introduced into the field of seismic damage and loss estimation.

Seismic vulnerability assessment of residential buildings was effectively taken up by Duzgun et al. (2011) and Bahadori et al. (2017) both at urban and city level, respectively. Lang et al. (2012) compared the earthquake loss estimates by empirical and analytical methods for Dehradun city. The economic losses and casualties varied between 12-36 billion INR and 915-2138 across two methods. Nanda et al. (2015) compared several loss estimation tools and estimated loss of life and property for institutional buildings of NIT Durgapur campus. Ghatak et al. (2017) computed the building damage, economic losses, and casualty estimates for Kolkata city. PGA and Pseudo Spectral Acceleration (PSA) values with a recurrence interval of 475 years were used for computation of losses. The expected economic losses and casualties were 231 billion INR and 3300, respectively. Wyss et al. (2017) estimated casualties for two Himalayan earthquakes, the M 7.9 Subansiri (1947) and M 7.8 Kangra (1905) earthquakes. The number of fatalities reported was 1.0 and 2.0 lakh for Subansiri and Kangra events, respectively. Wyss et al. (2018) computed the number of human losses and affected people in the case if Himalayan earthquakes of 1555 and 1505 should reoccur with the same magnitude and location. The estimates for 1555 and 1505 were 2.2 and 6.0 lakhs, respectively.

For hilly regions of the Indian Himalayas, the slope stability failure is the most common post-earthquake hazard, which can also be dealt in addition to the seismic hazard. An extensive two and three-dimensional stability analysis for seismically induced landslides were taken up by Zhou and Chen (2014), Zhou et al. (2015), Xu and Zhou (2018), Xu et al. (2017), and Zhou et al. (2019). For the readers who are working on multi-hazard analysis, the author urges to refer to these extensive studies. In this work, a site-specific seismic hazard for 2475 and 475 years return period, at 54 districts of Uttar Pradesh state (CIGP), is computed employing the ground motion equations of authors (Raghucharan et al. 2019). Utilizing the computed hazard levels at each district, seismic risk

in terms of damage probability of buildings, economic losses, and casualties are reported. Further, the sensitivity analysis is conducted to assess the relative influence of both parametric and model uncertainties.

2. Ground motion models

Seismic hazard assessment, damage and loss evaluation, and seismic resistant design of buildings at a location require site-specific response spectrum, which is acquired from ground motion models, also known as ground motion prediction equation (GMPE). In general, GMPEs were derived using regression technique utilizing either seismograph recordings, or artificial time histories, or a combination of both (Boore et al. 2008; Nath et al. 2009; Anbazhagan et al. 2013). The initial step in deriving an attenuation relationship is the presumption of functional form, which is bound to include inaccuracies in prediction (Gandomi et al. 2011).

Several existing GMPEs derived for India have only magnitude and distance as independent input parameters for anticipating the ground motion intensities, in contrary to robust ground motion models of NGA-West 2 project (Bozorgnia et al. 2014). Including many input parameters like GMPEs of NGA-West 2 project, for Indian locality, is not feasible due to the absence of precise acquisition of strong-motion data. Within the scope of recorded data from the Program for Excellence in Strong Motion Studies (PESMOS) and Central Indo-Gangetic Plains Network (CIGN) database, the GMPEs were developed by including a couple of other parameters: focal depth and average shear-wave velocity from the top to 30 m depth (Vs30), for improving the precision of the ground motion model.

Further, to overcome the model deficiencies due to assumption of functional form, authors employed ANN methodology to derive a relationship with earthquake magnitude (Mw), focal depth (FD), epicentral distance (R_{epi}), and average shear-wave velocity (V_{s30}) as input variables to anticipate the response spectrum ordinates at 0.01-4.0 s periods. Two site-specific ground-motion models derived by authors, one with recorded data of PESMOS and CIGN and another with combined recorded and synthetic data covering the data gap region of CIGP (Raghucharan et al. 2019) is employed to computed hazard in CIGP.

3. Seismic Hazard

The hazard evaluation of a region involves the identification of earthquake source models, which characterize the magnitude-frequency distribution, scaling relationships, and potential finite rupture geometries (Rong et al. 2017). The potential seismic sources around the study region, which can cause damage to the building and casualties, are identified and demarcated into six area source zone, as shown in Fig 1. The areas are discretized into grids of 50 km, and the source parameters are selected from literature (NDMA 2011; Nath et al. 2019) to model distributed seismicity. The intensity measure predicted was PGA and Sa at 25 periods [0.1, 0.2, 0.3, 0.4, 0.5, 0.55, 0.6, 0.65, 0.67, 0.7, 0.8, 0.9, 1.0, 1.1, 1.2, 1.3, 1.4, 1.5, 1.6, 1.7, 1.8, 1.9, 2.0, 3.0 and 4.0 s]. Table 1 shows the seismicity parameters of each source zone.

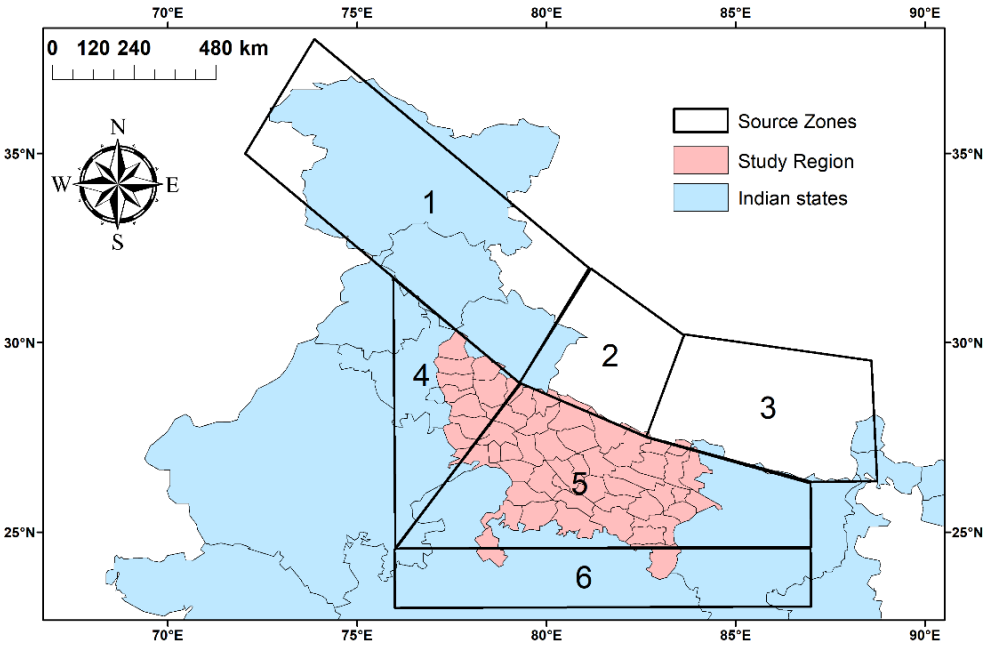

Fig 1. Map showing the study region (pink colour) and source zones considered for computing hazard in CIGP.

Table 1. Seismicity parameters selected for each zone.

Zone	a value	b value	Mmax	Reference
1	5.37	0.86	8.8	
2	3.15	0.69	7.8	NDMA (2011)
3	2.30	0.74	8.8	
4	2.79	0.69	7.2	
5	2.81	0.69	7.2	Nath et al. (2019)
6	2.86	0.73	7.0	

It also requires the selection of a reliable and accurate attenuation relationship for the region. Hence, region-specific ANN ground-motion models derived by authors (Raghucharan et al. 2019) is considered for computing seismic hazard for return periods of 475 and 2475 years for CIGP, India. The GMPEs are scripted in Python language within the OpenQuake engine platform for calculating hazard. Later the results are compared with the existing hazard values calculated by other researchers in CIGP to ascertain the predictions made in this study.

4. Seismic Risk

Earthquake loss estimation studies with site-specific hazard spectrum at 54 districts of Uttar Pradesh (CIGP) have been computed for the first time in this study. The Central Indo-Gangetic Plains (IGP) lying between the Himalayas and India shield region are contemplated as a zone of high risk due to thick soil deposits and adjacency to the highest seismic activity in India, the Himalayas. The sediments not only amplify the ground motions but also make foundations vulnerable to liquefaction. Hence, seismic risk assessment for the study region is of utmost essential. Seismic risk is computed by combining seismic demand, population exposure, and vulnerability (fragility) of buildings exposed.

4.1. Seismic Demand

Seismic demand for the study region is obtained from the site-specific response spectrum for each geographical unit (district) from the seismic hazard computed in this work. The spectral acceleration (Sa in g) values at 0.0, 0.1, 0.2, 0.3, 0.5, 0.75, 1.0, 1.5, and 2.0 s at bedrock are taken from the site-specific response spectrum for 2475 years return period, corresponding to MCE level. Soil amplification is addressed using the Vs30 parameter, which was obtained from Wald and Allen (2007). Fig 2 shows the map view of Vs30 values across all districts of the study region. Topographic amplification is neglected, as the CIGP is comprised of flat territory with a slope < 10°.

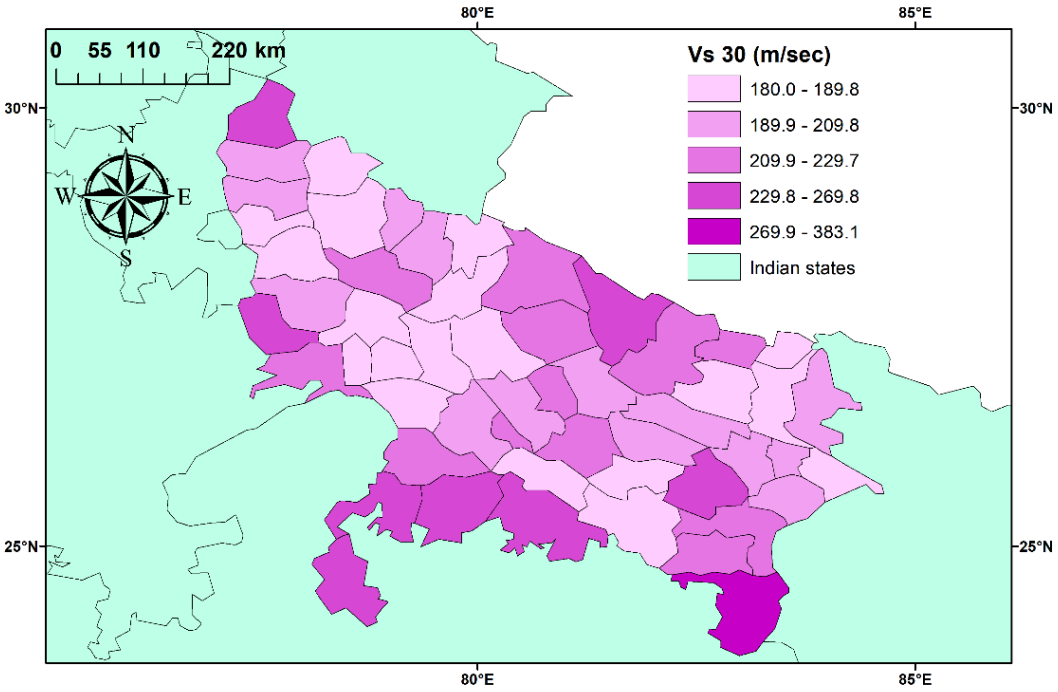

Fig 2. Shear wave velocity (Vs30) across 54 geo-units of the study area (Wald and Allen 2007). Light shade indicates loose soils, and thick shade represents rock strata.

4.2. Building Inventory and Population

The building inventory and population information of CIGP (54 geo-units of Uttar Pradesh state of India) are acquired from the Census of India (2011). The population density of all districts of the study region is represented in Fig 3. Building inventory details by predominant material used for roof and walls from Census (2011) are presented in Tables 2 and 3. Considering the construction practices prevailing in India, Prasad et al. (2009) designated 40 building classes based on wall, roof, framing types, and storey numbers. These building classes are accredited to 10 types and given nomenclature along with replacement cost of each building in rupees in Table 4 (Raghucharan and Somala 2018). Also, Tables 2 and 3 are united to give the percentage of houses at all geo-units to these model building types (MBTs), as shown in Table 5. The MBTs are categorized into ten types for assigning vulnerability functions based on the material and type of construction followed.

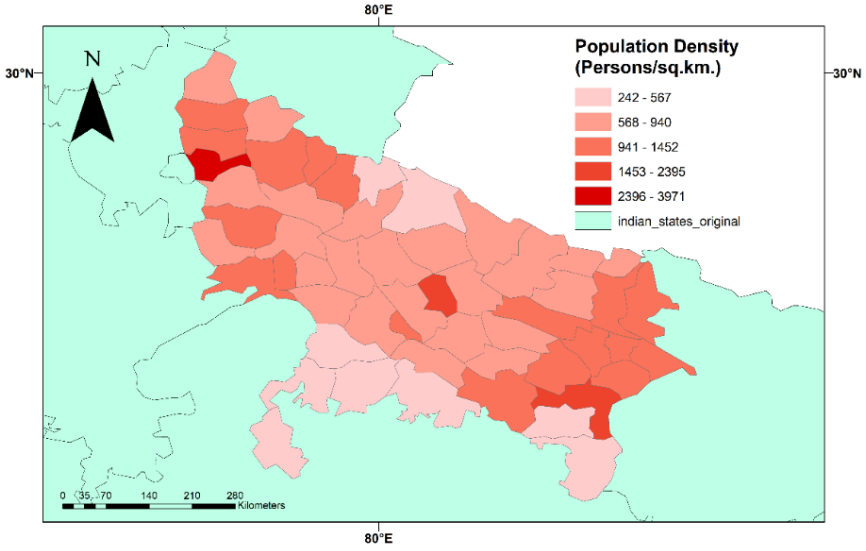

Fig 3. Map view of population density across 54 geo-units of the study area. The density of the region increases with an increase in colour shade.

Table 2. Distribution of households by predominant material of roof as per the Census of India, 2011.

India/ State/ Union Territory	Distribution of households by predominant material of the roof										
	Total No. of Households (Excluding institutional households)	Grass, Thatch, Bamboo, Wood, Mud, etc.	Plastic, Polythene	Tiles			Brick	Stone/slate	G.I. Metal, Asbestos sheets	Concrete	Any other material
				Handmade Tiles	Machine-made Tiles	Total					
Uttar Pradesh	32924266	23.3	0.5	8.7	8.1	0.6	32.8	13.9	2.9	17.6	0.4

Table 3. Distribution of households by predominant material of wall as per the Census of India, 2011.

India/ State/ Union Territory	Distribution of households by predominant material of Wall										
	Total No. of Households (Excluding institutional households)	Grass, Thatch, Bamboo, etc.	Plastic, Polythene	Mud, Unburnt brick	Wood	Stone			G.I. Metal, Asbestos sheets	Burnt brick	Concrete	Any other material
						Total	Not packed with mortar	Packed with mortar				
Uttar Pradesh	32924266	5	0.3	20	0.1	3.2	1.2	2	0.1	68.4	0.6	2.4

Table 4. Classification of each Model Building type along with their replacement cost selected in the study (10 in total).

Model Building Class	Nomenclature	Replacement cost in Rupees, per m^2
AMM	Adobe Mud Mortar walls with Temporary roof	4500.0
ALC	Adobe lime and cement Mortar walls with Temporary roof	4500.0
MMB	Mud Mortar Bricks with Temporary roof	8937.5
BTR	Bricks and tiles roof	8937.5
BSR	Bricks and stone roof	8937.5
BCM	Bricks in cement mortar for walls and roof	8937.5
BMS	Bricks wall with metal sheet roof	8937.5
BCS	Bricks wall with concrete slab	10350.0
RCL	Reinforced wall and slab-low rise	10350.0
RCM	Reinforced wall and slab-medium rise	10350.0

Table 5. Distribution of Houses in all districts of Uttar Pradesh (Census 2011) to Standard Model Building types adopted from Prasad et al. (2009).

Total Houses/ households	Distribution of households by predominant material of the wall									
32924266	Grass, Thatch, Bamboo, Plastic, Polythene, Wood, Mud, Unburnt bricks, etc.	Stone Packed with mortar	Burnt Bricks						Concrete	
% of Households	29	2	68.4						0.6	
Distribution based on the material of Roof	NIL	NIL	Grass, Thatch, Bamboo, Wood, Mud, Plastic, Polythene, others, etc.	Tiles: Handmade and Machine made	Stone/ Slate	Bricks	G.I, Metal, Asbestos Sheets	Concrete	NIL	NIL
% of Households	29	2	24.1	8.7	13.9	32.8	2.9	17.6	25	75
Model Building Type (MBT) classification	AM11, AM21	AL11, AL21, AL31, AC11, AC21, AC31	MM11, MM21, MM31	ML11, ML21, ML31	ML12, ML22, ML32	MC11, MC21, MC3L1	MC12, MC22, MC3L2	MC3M	RC1L	RC1M
% of Total Houses	29.00	2.00	16.48	5.95	9.51	22.44	1.98	12.04	0.15	0.45
MBT code	AMM	ALC	MMB	BTR	BSR	BCM	BMS	BCS	RCL	RCM

4.3. Fragility Functions

HAZUS-MH database provides fragility functions for different model building classes that are useful for computing damage probability and socio-economic losses. As the construction methodologies for building inventory in India vary noticeably from buildings of the United States (US), fragility functions recommended in HAZUS-MH (FEMA 2003) cannot be applied directly. Analytical capacity and fragility functions shall be meticulously chosen since they will bear a substantial impact on the risk and loss results (Lang et al. 2012). The capacity and fragility functions (Vulnerability functions) of the 10 Model Building types (MBTs) are obtained from Cattari et al. 2004, Kappos and Panagopoulos (2008, 2010), Prasad 2010.

For buildings typologies made of adobe materials and rubble stone (MBT 1-2 in Table 4), vulnerability functions are unavailable for India. Hence, these curves are adopted from Italian conditions (Cattari et al. 2004) due to the resemblance they exhibit in terms of ingredients used in construction. For building types made of mud mortar and clay in brick masonry, MM, ML, and MC, curves derived by Prasad (2010) by suitably consideration of construction practices in north India are adopted for MBTs 3-8. For MBTs 9-10, the curves provided by Kappos and Panagopoulos (2008, 2010) with fully-infilled reinforced concrete (RC) frame buildings are chosen for RC low (1 to 3 storey) and Mid-rise (4 to 7 storey). Since a large number of the buildings in the CIGP region are constructed before code or by breaching the IS code guidelines, the low-code/pre-code conditions can be applied. Table 6 presents the capacity and fragility function values for four damage states: slight, moderate, extensive, and complete, for all ten building types, along with their reference.

Table 6. Vulnerability functions adopted for different types of building in the CIGP region. Capacity values are specified at yield and ultimate, while the fragility values are reported as mean spectral displacement and standard deviation for four damage states (slight, moderate, extensive, and complete). The reference is provided in the last column.

Model Building Class	Building Type	Stories	Capacity curve parameters (Yield and Ultimate Points)				Fragility Function parameters for damage states (slight, moderate, extensive and complete)								Reference
			Dy (mm)	Ay (m/s2)	Du (mm)	Au (m/s2)	Sd_{slight} (mm)	β_{slight}	Sd_{mod} (mm)	β_{mod}	Sd_{ext} (mm)	β_{ext}	Sd_{comp} (mm)	β_{comp}	
AMM	AM11, AM21, AM12, AM22	1	1.01	1.408	10.70	1.408	0.64	1.11	1.36	1.11	5.85	1.11	10.80	1.11	Cattari et al. (2004)
ALC	AL11, AL21, AL31, AC11, AC21, AC31	1	1.01	2.288	11.10	2.288	0.64	1.13	1.37	1.13	6.06	1.13	11.20	1.13	
MMB	MM11, MM21, MM31	1	1.50	1.079	8.40	1.472	1.30	0.80	2.30	0.90	4.10	0.90	8.00	1.05	Prasad (2010)
BTR	ML11, ML21, ML31	1	1.00	1.570	8.30	2.158	0.90	0.80	1.80	0.90	4.00	0.90	8.00	1.05	
BSR	ML12, ML22, ML32	2	2.60	1.275	14.60	1.766	2.20	0.80	4.00	0.90	7.80	0.90	14.40	1.05	
BCM	MC11, MC21, MC3L1	1	1.30	1.962	8.00	2.453	1.10	0.80	2.00	0.90	4.10	0.90	8.00	1.05	
BMS	MC12, MC22, MC3L2	2	2.60	1.570	14.60	2.158	2.20	0.80	4.50	0.90	7.70	0.90	14.00	1.05	
BCS	MC3M	3+	2.60	1.570	14.60	2.158	2.20	0.80	4.50	0.90	7.70	0.90	14.00	1.05	
RCL	RC1L	1-3	4.90	3.237	51.10	3.924	3.40	0.41	7.30	0.62	28.00	1.04	51.10	1.32	Kappos and Panagopoulos (2008, 2010)
RCM	RC1M	4-7	10.30	2.256	68.00	2.943	7.20	0.38	15.40	0.54	39.10	0.86	68.00	1.09	

NORSAR and the University of Alicante have developed SELENA, a MATLAB (2017) based tool with a fundamental methodology adopted from HAZUS. SELENA computes damage probability of buildings, economic outlay, and human casualties using an analytical method, as explained in Molina et al. (2010).

4.4. Seismic Damage and Losses

4.4.1. Damage Probability

In order to evaluate the probability of damage of a building, the spectral displacement value, which is the point of intersection (performance point) of capacity and demand curve, shall be identified (Molina et al. 2015). At present, SELENA has introduced three methods for computing the performance point, the capacity spectrum method (CSM) (ATC, 1996; FEMA, 1997), the modified capacity spectrum method (MADRS), and the improved displacement coefficient method (I-DCM) (FEMA, 2005). Since the I-DCM methodology is an improved version of the three, this methodology is selected for computing the performance point of each model building class in the CIGP region.

Seismic performance point based on I-DCM, for a given capacity and demand curve, is determined according to the following methodology. The capacity curve for a given MBCs is generated, and the effective time period of the system is computed as:

$$T_{eff} = 2\pi \sqrt{\frac{D_y}{A_y}} \qquad (1)$$

The spectral acceleration for the corresponding linear SDOF system, S_a^{es} can be read from the demand curve for the obtained effective time period (Teff). From the obtained S_a^{es}, the peak elastic spectral displacement demand S_d^{es} is computed from:

$$S_d^{es} = \frac{T_e^2}{4\pi^2} . S_a^{es} \qquad (2)$$

The performance point is then computed as:

$$\Delta_p = C_1 . C_2 . S_d^{es} \qquad (3)$$

Where C1 and C2 are modification factors given in FEMA-440 (FEMA, 2005).

After computing the maximum displacement demand (performance point) for each model building class, the fragility functions which represent spectral displacement (median value) and standard deviation, for each structural damage case (slight, moderate, extensive and complete) of each model building class are selected from literature (Table 6). By overlaying the maximum displacement demand (performance point value) on fragility curves, damage probability for five different damage states (including None) can be obtained, as illustrated in Figure 4. From the damage probability of each damage state, the damage results are obtained with respect to the number of damaged buildings, or building floor area of each damaged building class.

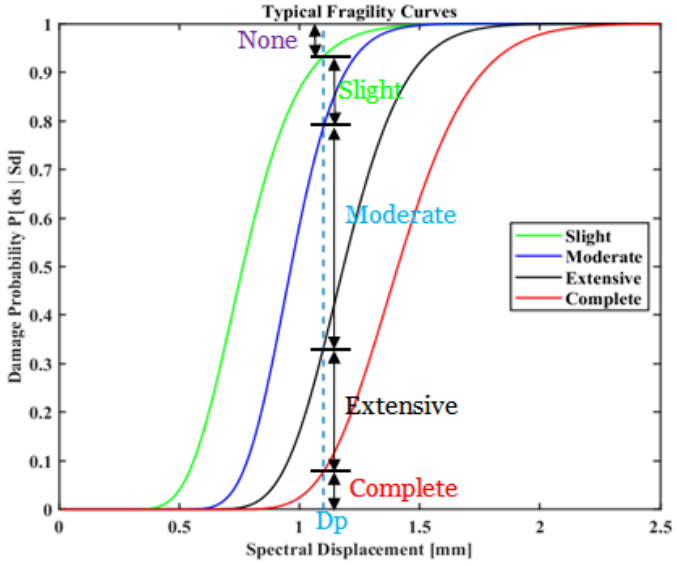

Fig 4. Typical fragility curves showing the damage probability of each damage cases (None, Slight, Moderate, Extensive, and Complete) for a given maximum displacement demand, Dp

4.4.2. Economic Losses

The economic losses induced by structural damage at a given geo-unit, in user-defined input currency, is computed when the building inventory data is provided in terms of building floor area. The economic losses covering slight and moderate damage states (for the repair of the building) and extensive and complete (for replacement) are computed using equation 4.

$$E_{loss} = R_{cm} . \sum_{k=1}^{N_{ot}} \sum_{l=1}^{N_{bt}} \sum_{m=1}^{N_{ds}} BA_{k,l} . DP_{l,m} . CR_{k,l,m} \qquad (4)$$

N_{ot} indicates the types of occupancy; N_{bt} refers to building typologies, N_{ds} refers to damage states ds, in numbers. R_{cm} indicates the regional cost multiplier, which is introduced to account for cost variation across geographical units, the terms $BA_{k,l}$ denotes, built area of the MBT, l in the occupancy type k; $DP_{l,m}$ indicates the probability of damage for each structural damage m for MBT, l and $CR_{k,l,m}$ indicates repair or replacement cost in the given input currency for structural damage m, for the type of occupancy k and MBT, l.

The cost of replacement of building model classes was adopted from Lang et al. (2012), which was derived based on the field data collected in the different socio-economic clusters in Dehradun. Since Dehradun, lying in Uttarakhand state, was part of Uttar Pradesh state of India till its bifurcation in the year 2000, the same replacement cost is considered appropriate for this study. Since most of the economic clusters that prevail in India are occupied by low income and middle-income groups, the total replacement cost (sum of structural, non-structural and contents cost) is taken as the average of those income groups and is represented in Table 4 along with nomenclature of buildings. As the cost variation across geo-units was not considered in the present study, R_{cm} is set to 1.0 in the calculations. Due to lack of data, the cost for other damage states, slight, moderate, and extensive is adopted from HAZUS-MH (FEMA 2003) as 2, 10, and 50 percent of complete damage, respectively. Another useful parameter for comparing the risk across geo-units is the Mean Damage ratio (MDR) (FEMA 2003). It is the ratio of cost corresponding to each damage state, to the cost of new construction. The damage ratio is computed in two forms: (i) for each geo-unit for all model building classes known as MDR and (ii) for each model building class and all geo-units known as MDR total.

4.4.3. Human Casualties

The human casualties are computed based on the simplified formula based on Coburn and Spence (2002) and accordingly modified to incorporate the injury level as:

$$C_i = C_l^{sd} + C_l^{nd} + C_l^{in} \quad (5)$$

The terms C_l^{Sd} denotes, number of injuries/deaths occurring due to structural damage for each injury level, l; C_l^{nd} denotes number of injuries/deaths occurring due to non-structural damage for each injury level, l; and C_l^{in} indicates number of injuries/deaths due to earthquake induced threats, such as fires, floods, landslides etc., for each injury level, l.

Where l represents the four levels of severity, light (l = 1), moderate (l = 2), heavy (l = 3), and death (l = 4).

SELENA v6.5 estimates human losses generated from structural damage only. Human losses due to non-structural damage imply death due to falling off shelves, fans, woodwork, electronic appliances, etc., are assumed to be rare and hence neglected. In view of considering the occupancy cases which depends strongly on the portion of the day, the number of injuries/deaths are calculated at early hours (2:00 AM), day time (10:00 AM) and rush hours (5:00 PM) to generate highest number of casualties for the people at home (early hours), the people at work (day time) and the people during commuting time (rush hour).

5. Sensitivity Analysis

In the present study, sensitivity analysis is conducted to find out the relative influence of each independent parameter like moment magnitude, epicentral location, focal depth, strike, dip, and ground motion model (GMPE) on the economic and human losses.

Since the CIGP falls between Kangra earthquake of 1905 and Nepal earthquakes occurred in 2015, with a future expected earthquake of Mw > 8.0 (Bilham et al. 1995; Khattri 1999; Rajendran and Rajendran 2005; Bilham and Wallace 2005; Rajendran et al. 2015; Li et al. 2019), the magnitude (Mw) is varied between 7.5 and 8.5 with an average value of 8.0. Further, to select the location of scenario earthquakes, the seven hundred km long segment between the rupture areas of Kangra and Nepal events is divided into four relatively equal segments. The range of focal depth, strike, and dip values are selected from the historic earthquakes data of the region (Table 7).

Table 7. Source parameters of historic earthquakes in the study region and the data source.

Earthquake	Magnitude (Mw)	Latitude	Longitude	Focal Depth	Strike	Dip	Focal Mechanism	Source
1991 Uttarkashi	6.8	30.22	78.24	15.0	317	14	Thrust	Global CMT solutions
1999 Chamoli	6.5	30.38	79.21	15.0	280	7	Thrust	Global CMT solutions
1934 Bihar-Nepal	8.1	26.45	86.25	10	-	6	Thrust	Hough and Roger (2008)
1905 Kangra	7.8	32.00	76.75	11	-	6	Thrust	Hough and Roger (2008)

The six uncertainty variables examined in the sensitivity analysis are presented in Table 8, along with their range, and base model values (median values). The Two GMPEs derived by authors for Indo-Gangetic plains (GMPE-1 and GMPE-2) were adopted independently and with 0.5 factor each to verify the effect of model dependency on loss estimations. The scenario events locations selected for sensitivity analysis and significant events that occurred in IGP are shown in Fig 5.

Table 8. Range and median values of parameters considered in the sensitivity analysis.

Parameter Name	Range [Trail values]	Median Value [Base Model]
Focal Depth (km)	10-15 [10, 12.5, 15]	12.5
Strike	275-325 [275, 300, 325]	300
Dip	5-15 [5, 10, 15]	10
Epicentre Location	3 locations (Latitude, Longitude) on a 700 km stretch between 1905 Kangra and 2015 Nepal earthquakes dividing the gap into four segments. [(29.815,78.556); (28.654,81.221); (27.341,83.848)]	28.654,81.221
Moment Magnitude	7.5 to 8.5 (7.5, 8.0, 8.5)	8.0
GMPEs	ANN GMPE-1 & ANN GMPE-2 [a,b,c] a. GMPE-1 b. 0.5 GMPE-1 and 0.5 GMPE-2 c. GMPE-2]	0.5 GMPE-1 and 0.5 GMPE-2

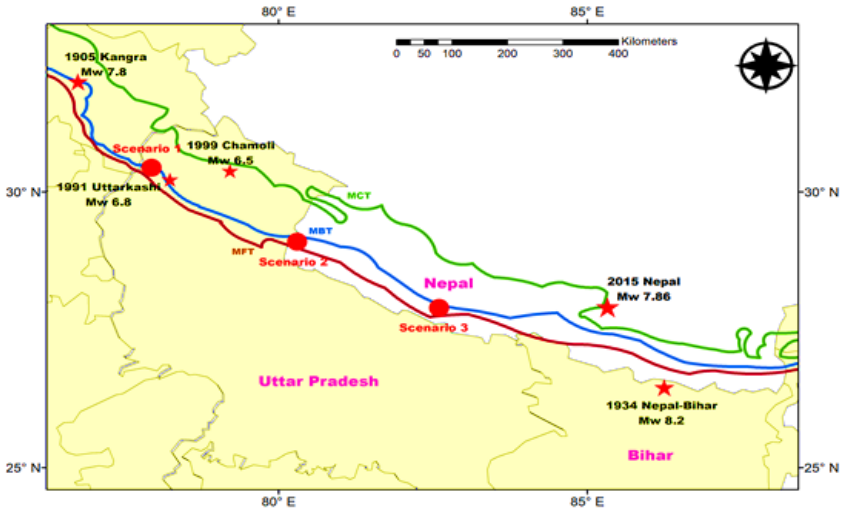

Fig 5. Plot showing the location of scenario earthquakes along with significant earthquake events occurred in the Himalayas.

6. Results and Discussions

The seismic hazard is computed for 2% and 10% probability in 50 years, covering 54 districts of the CIGP region by employing the two GMPE models derived by authors. Fig 6 shows the seismic hazard across the study region for 10 % and 2 % probability of exceedance in 50 years in terms of PGA and PSA at 0.2 and 1.0 s, respectively. These results are validated using the previous works on hazard available in the literature at certain cities (Meerut, Agra, Kanpur, Lucknow, Allahabad, and Varanasi) in the CIGP (Table 9). The prediction of hazard from the ANN-based GMPEs derived in this study is comparable with the estimates by other researchers. The computed intensity levels are used to evaluate seismic risk in CIGP. Figure 6 implies that the north-western districts of Uttar Pradesh state have high seismic hazard as the main frontal thrust is passing along these regions (indicated by brown colour in Fig. 6). Districts farther from the three major fault line of Himalayas, MBT, MCT and MFT are seismically least critical.

Further, from Table 9, it can be seen that only Nath et al. (2019) predicted higher values at both Lucknow and Varanasi, compared to the works of other researchers, which may be due to the fact that the attenuation relationship was derived considering only Nepal 2015, Nepal-Bihar 1934 and Jabalpur earthquakes which are in proximity to the study region. Also, a GMPE which does not belong to India, Abrahamson, and Silva (2008) was included in calculating the hazard. Hence, the site-specific hazard values computed in this research are considered for computing seismic risk at the district level in CIGP.

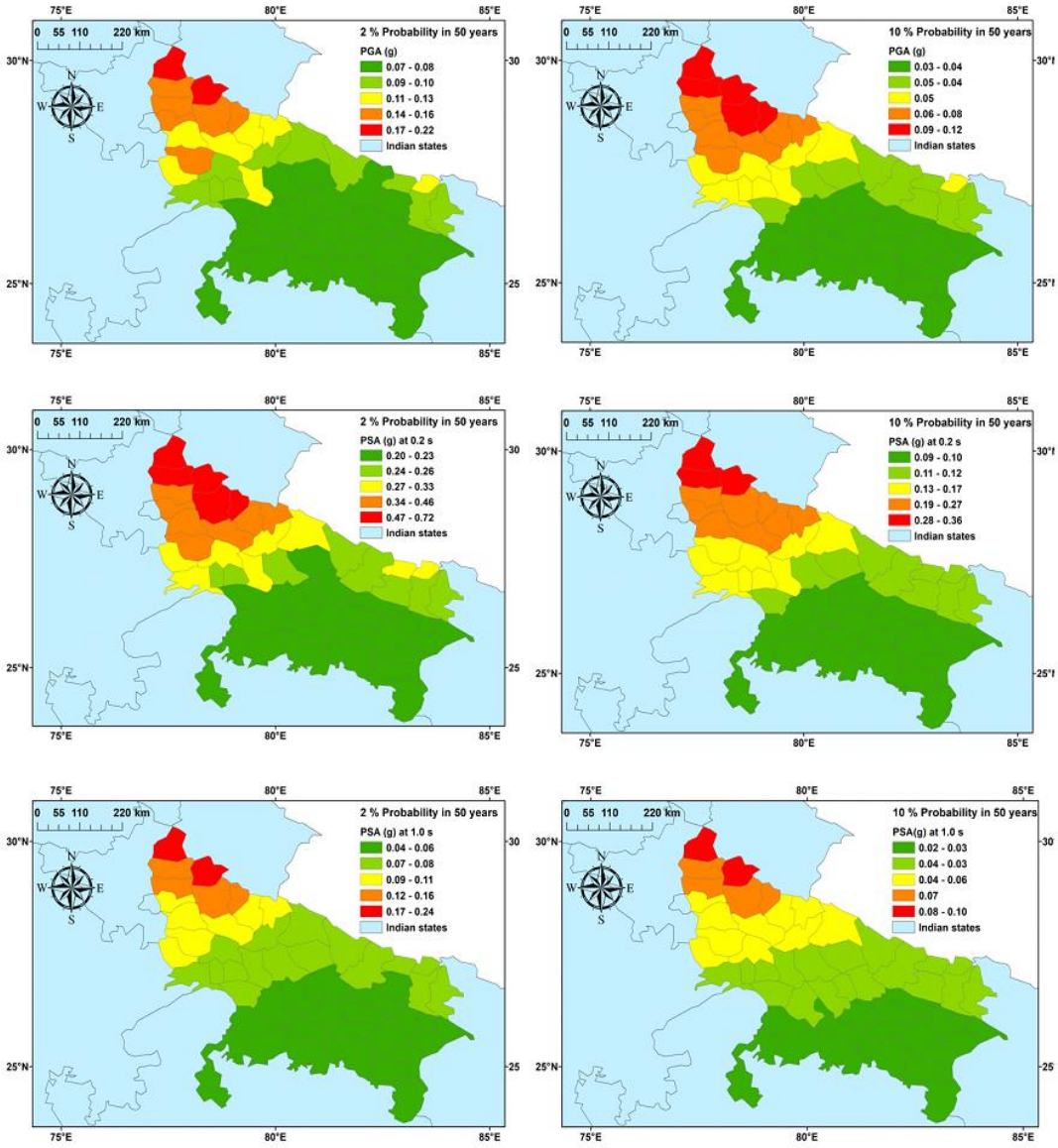

Fig 6. Seismic hazard distribution across 54 geo-units of Uttar Pradesh state in terms of PGA, PSA at 0.2 s and PSA at 1.0 s at the rock, for 475 and 2475 return period.

Table 9. Comparison of PGAs at 10% probability of exceedance in 50 years between different studies at six important cities.

Reference	PGA at 10 % probability in 50 years					
	Meerut	Agra	Kanpur	Lucknow	Allahabad	Varanasi
Khattri et al. (1984)	-	-	-	0.05	-	0.05
Bhatia et al. (1999)	-	-	-	0.08	-	0.06
NDMA (2011)	0.06	0.06	0.03	0.04	0.03	0.02
Kumar et al. (2013)	-	-	-	0.04-0.07	-	-
Sitharam and Kolathayar (2013)	-	-	-	0.06-0.12	-	0.05-0.09
Nath et al. (2019)	-	-	-	0.17-0.18	-	0.09-0.11
This study	0.08	0.05	0.03	0.04	0.03	0.03

Seismic risk in terms of building damage and loss is computed for 54 districts (geo-units) of the CIGP region for a MCE (2% probability in 50 years). Fig 7 emphasizes the average damage probability of ten model building types across all geo-units, for five damage states: None, Slight, Moderate, Extensive, and Complete. The figure confirms that out of ten building types, four (MMB, BSR, BMS, and BCS) have a high probability of complete damage. This affirms that inventories existing in CIGP have a high probability of collapse due to the transient type of construction, which need immediate retrofitting / replacement measures to curb financial cost and human losses. Further, model building type, MMB (Table 4), covering 16.5 % of total households, has a maximum collapse rate of nearly 60%. Also, for each model building type, by multiplying the percentage of buildings with the collapse probability, the total buildings in CIGP that might collapse for MCE and DBE earthquakes are 36% and 11%, respectively.

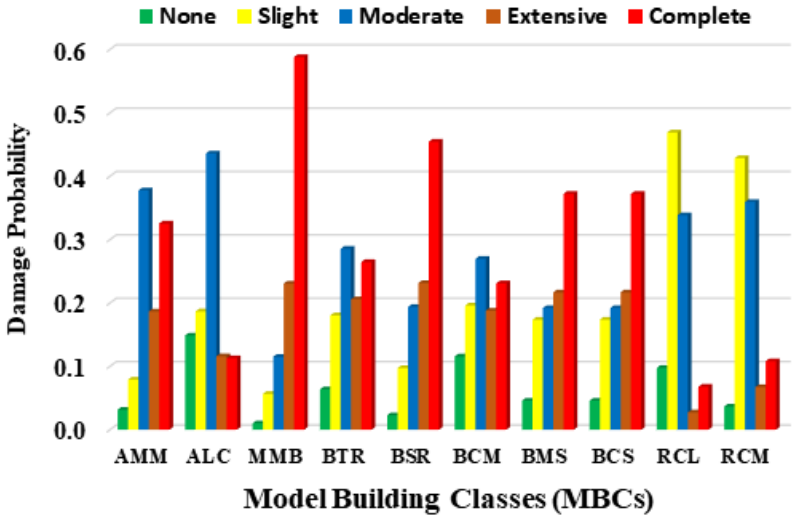

Fig 7. Histogram plot of the damage probabilities of ten model building types adopted in this research at five damage states: None, Slight, Moderate, Extensive, and Complete.

Further, the Geo-Unit Allahabad, which falls under seismic zone II of IS 1893:2016, is identified by loose soils with average V_{s30} of 185 m/s with the highest population among other geo-units. Our results acknowledge that Allahabad has expected economic losses (Fig 8) around 16 billion dollars and the maximum number of homeless (Fig 9) and uninhabitable dwellings (Fig 10). These findings will drive policymakers and re-insurance corporations to reassess their approach and action plan.

For an MCE (2% in 50 years) and Design Basis Earthquake (DBE) (10 % in 50 years), the anticipated human losses are about 12 and 4 lakhs respectively that are principally arising at night time (2:00 AM) (Fig 11 and the predicted economic outlay is around 630 and 270 billion dollars respectively.

During sensitivity analysis, the output variables monitored are economic and human losses. These are represented as Pie diagrams and Tornado plots.

Fig 12 represents a pie diagram showing the proportion of each sensitivity parameter to the total uncertainty in computing financial and human losses. The magnitude of the earthquake is highly sensitive, followed by source location.

The range of outputs for the assumed range of each input parameter can be represented by a tornado plot, which gives the two boundary values, known as swing. The swing is denoted as the range of sensitivity of output values for the adopted range of inputs. The greatest swing was noticed for the variable magnitude, followed by source location (Fig 13).

From the sensitivity study, we conclude that magnitude followed by source location, GMPE, and focal depth, respectively, are in the order of high to low sensitivity. For the probable magnitude range of Mw 7.5 to 8.5, the expected economic outlay might vary between 60 and 150 billion dollars, and the human losses might vary from 0.8 to 2.8 lakhs, respectively.

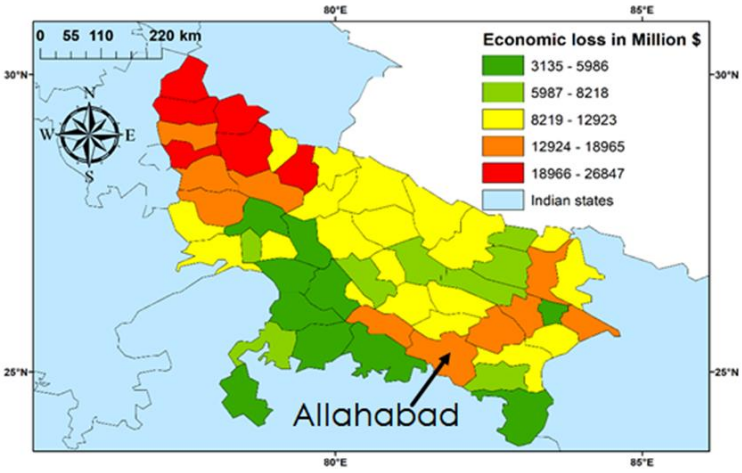

Fig 8. The anticipated economic outlay in the study area (CIGP) for MCE, with Allahabad district indicated by an arrow mark.

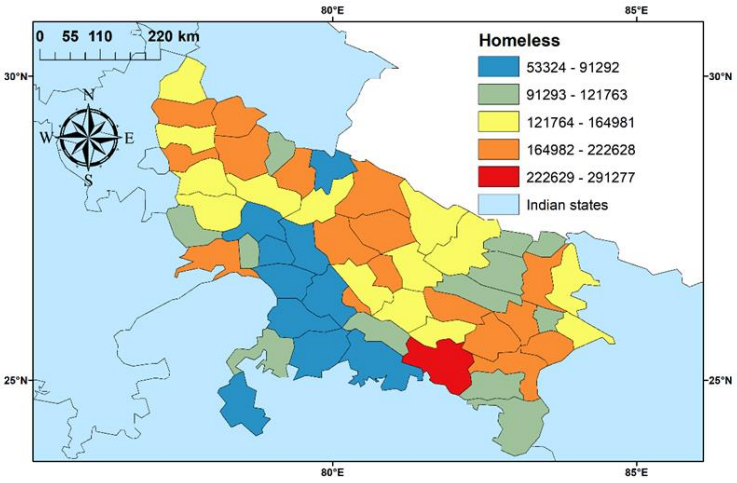

Fig 9. Allahabad district characterized by the maximum number of Homeless in the study area (CIGP) for MCE.

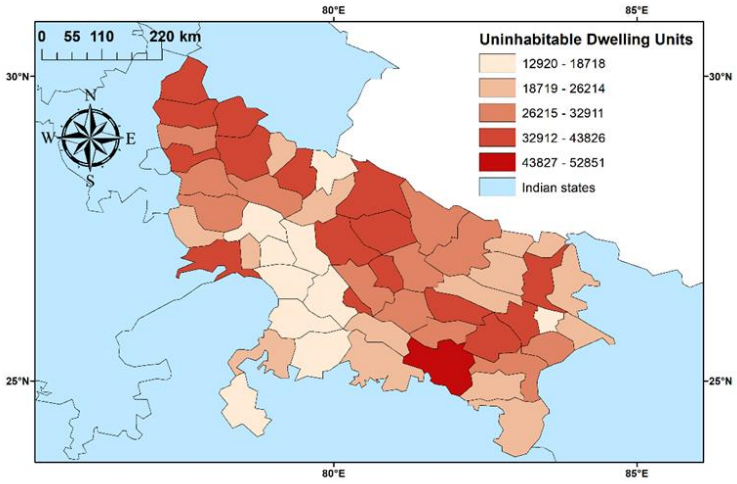

Fig 10. The maximum number of uninhabitable dwelling units recorded in Allahabad district, in the study area (CIGP) for MCE.

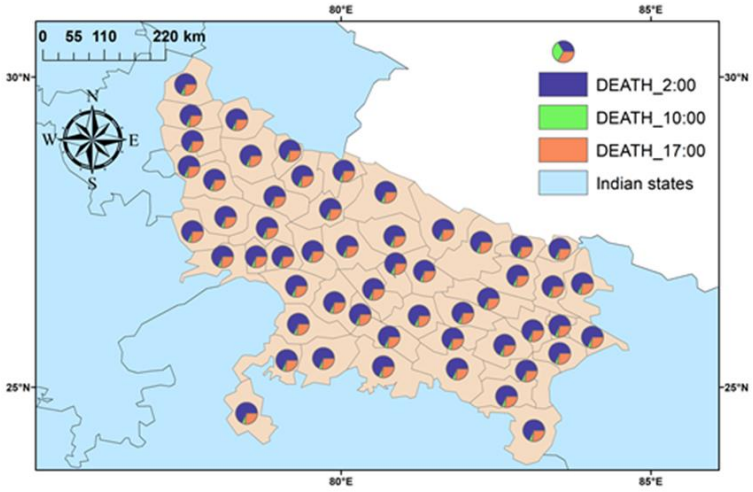

Fig 11. Pie chart representing the human losses at 2 AM, 10 AM and 5 PM in a day, at all geo-unit of the study region, dominated at 2 AM.

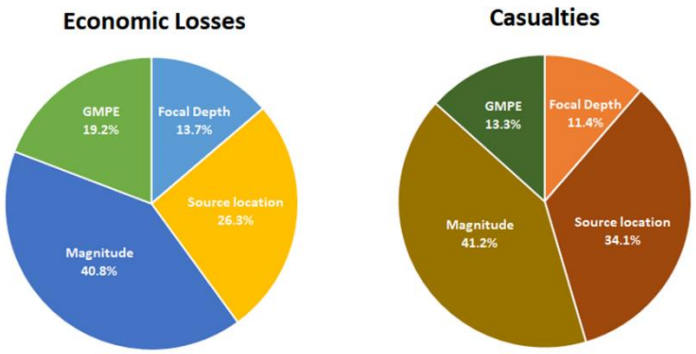

Fig 12. Pie diagram depicting the contribution of input parameters for computed economic and human losses in the study area, dominated by magnitude followed by GMPE.

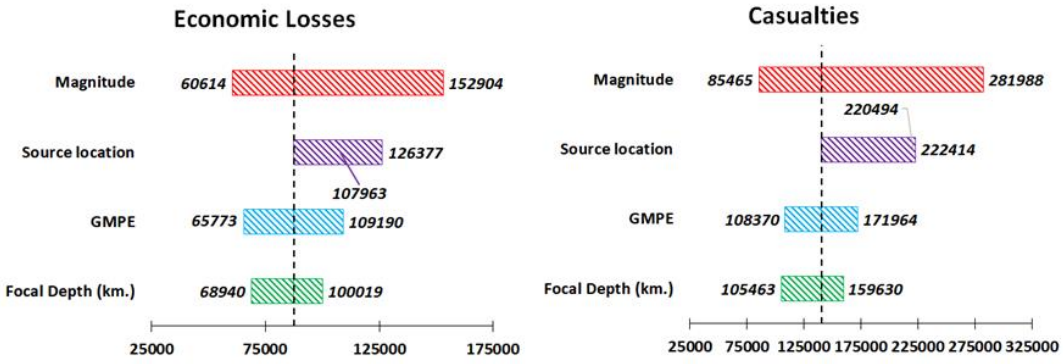

Fig 13. Tornado plots depicting the deviation in economic and human losses from the median (dotted line) for all parameters considered, dominated by magnitude followed by GMPE.

7. Conclusions

Site-specific seismic hazard and earthquake loss estimation studies were computed for residential buildings in 54 geo-units (districts) of Uttar Pradesh state in India, covering the CIGP region. The key findings for effective disaster mitigation are as follows:

- For the first time, the seismic hazard spectrum in terms of PGA and PSA (5% damping) at 25 periods for a return period of 475 and 2475 years is computed on a large scale at each district of Uttar Pradesh (54 in total).
- Earthquake loss estimation in terms of damage probability of building in entire CIGP, economic losses, and casualties in each district is reported for the first time in this study
- The results from this study reveal that Model Building types, MMB (Mud Mortar Bricks with temporary roof) consisting of 16.5% of total buildings have the highest collapse probability of nearly 60%.
- Further, brick walls with stone roof (BSR) and brick walls with metal sheet roof (BMS) also have high extensive and collapse damage compared to other building groups. These three building typologies, which are located in the seismically critical region and proximity to the Himalayas, need immediate retrofitting/replacement
- Geo-unit Allahabad, even though lying in zone II as per IS 1893:2016, has the most number of homeless and uninhabitable dwellings due to the presence of poor soils. This finding will give insight to future rehabilitation and resettlement centers.
- For a future earthquake of magnitude between Mw 7.5 to 8.5, the expected economic outlay might vary from 60 to 150 billion dollars, and the human losses might vary between 0.8 and 2.8 lakhs.

The methodology of seismic risk assessment described in this study may be generalized to any study region in the world if seismic demand, building inventory data, and fragility functions of buildings are available.

Acknowledgements

Surendra Nadh Somala acknowledges the funding from DST project INT/RUS/RFBR/P-335.

References

Abrahamson N, Silva W (2008) Summary of the Abrahamson & Silva NGA ground-motion relations, *Earthquake spectra* 24:67-97.

Anbazhagan P, Kumar A, Sitharam TG (2013) Ground motion prediction equation considering combined dataset of recorded and simulated ground motions, *Soil Dynamics and Earthquake Engineering* 53:92-108.

ATC A 40 (1996) Seismic evaluation and retrofit of concrete buildings. Applied Technology Council, report ATC-40. Redwood City.

Atkinson GM, Boore DM (2006) Earthquake ground-motion prediction equations for eastern North America, *Bulletin of Seismological Society of America* 96:2181-2205.

Bagchi S, Raghukanth STG (2017) Seismic Response of the Central Part of Indo-Gangetic Plain, *Journal of Earthquake Engineering* 23:183-207.

Bahadori H, Hasheminezhad A, Karimi A (2017) Development of an integrated model for seismic vulnerability assessment of residential buildings: Application to Mahabad City, Iran, *Journal of Building Engineering* 12:118-31.

Basu S, Nigam NC (1977) Seismic risk analysis of Indian peninsula. In Proceedings of sixth world conference on earthquake engineering, *New Delhi* 1:782–788.

Bhatia SC, Kumar MR, Gupta HK (1999) A probabilistic seismic hazard map of India and adjoining regions.

Bilham R (2009) The seismic future of cities, *Bulletin of Earthquake Engineering* 7:839.

Bilham R, Bodin P, Jackson M (1995) Entertaining a great earthquake in western Nepal: historic inactivity and geodetic tests for the present state of strain, *Journal of Nepal Geological Society* 11:73-78.

Bilham R, Wallace K (2005) Future Mw> 8 earthquakes in the Himalaya: implications from the 26 Dec 2004 Mw= 9.0 earthquake on India's eastern plate margin, *Geological Survey of India Special Publication* 85:1-4.

BIS (Bureau of Indian Standards) (2016) Indian Standard Criteria for Earthquake Resistant Design of Structures: General Provisions and Buildings, IS 1893-Part 1, Fifth Revision. BIS, New Delhi, India.

Boore DM, Atkinson GM (2008) Ground-motion prediction equations for the average horizontal component of PGA, PGV, and 5%-damped PSA at spectral periods between 0.01 s and 10.0 s, *Earthquake Spectra* 24:99-138.

Bozorgnia Y, Abrahamson NA, Atik LA, Ancheta TD, Atkinson GM, Baker JW, Baltay A, Boore DM, Campbell KW, Chiou BSJ, Darragh R (2014) NGA-West2 research project, *Earthquake Spectra* 30:973-987.

Campbell KW, Bozorgnia Y (2003) Updated near-source ground-motion (attenuation) relations for the horizontal and vertical components of peak ground acceleration and acceleration response spectra, *Bulletin of Seismological Society of America* 93:314-331.

Cattari S, Curti E, Giovinazzi S, Lagomarsino S, Parodi S, Penna A (2004) A mechanical model for the vulnerability assessment of masonry buildings in urban areas. In Proceedings of the VI Congreso nazionale "L'ingegneria Sismica in Italia", Genova, Italy

Chadha RK, Srinagesh D, Srinivas D, Suresh G, Sateesh A, Singh SK, Pérez-Campos X, Suresh G, Koketsu K, Masuda T, Domen, K (2015) CIGN, a strong-motion seismic network in central Indo-Gangetic plains, foothills of Himalayas: First results, *Seismological Research Letters* 87:37-46.

Cornell CA (1968) Engineering seismic risk analysis, *Bulletin of Seismological Society of America* 58:1583-1606.

Das S, Gupta ID, Gupta VK (2006) A probabilistic seismic hazard analysis of northeast India, *Earthquake Spectra* 22: 1-27.

Duzgun HS, Yucemen MS, Kalaycioglu HS, Celik KE, Kemec S, Ertugay K, Deniz A (2011) An integrated earthquake vulnerability assessment framework for urban areas, *Natural hazards* 59(2):917-47.

Federal Emergency Management Agency FEMA (1997) NEHRP Guidelines for the Seismic Rehabilitation of Buildings, FEMA 273, Washington DC, United States.

Federal Emergency Management Agency FEMA (2000). commentary for the seismic rehabilitation of buildings (FEMA356). Washington, DC: Federal Emergency Management Agency, 7.

Federal Emergency Management Agency FEMA (2003) HAZUS-MH. Multi-hazard Loss Estimation Methodology, Technical manual., Washington DC, United States.

Federal Emergency Management Agency FEMA (2005) Improvement of nonlinear static seismic analysis procedures, FEMA 440. Technical report, Applied Technology Council, California, United States.

Freeman SA (1975) Evaluations of existing buildings for seismic risk-A case study of Puget Sound Naval Shipyard. In Proc. 1st US National Conference on Earthquake Engineering, Bremerton, Washington: 113-122.

Freeman SA (1978) Prediction of response of concrete buildings to severe earthquake motion. Special Publication 55:589-606.

Gandomi AH, Alavi AH, Mousavi M, Tabatabaei SM (2011) A hybrid computational approach to derive new ground-motion prediction equations, *Engineering Application of Artificial Intelligence* 24:717-732.

Ghatak C, Nath SK, Devaraj N (2017) Earthquake induced deterministic damage and economic loss estimation for Kolkata India, *Journal of Rehabilitation in Civil Engineering* 5:1-24.

Ghosh B, Pappin JW, So MML, Hicyilmaz KMO (2012) Seismic hazard assessment in India. In Proc. of the Fifteenth World Conference on Earthquake Engineering-2012.

Jaiswal K, Sinha R (2007) Probabilistic seismic-hazard estimation for peninsular India, *Bulletin of Seismological Society of America* 97:318-330.

Kappos AJ, Panagopoulos G, Penelis GG (2008) Development of a seismic damage and loss scenario for contemporary and historical buildings in Thessaloniki, Greece, *Soil Dynamics and Earthquake Engineering* 28(10-11):836-50.

Kappos AJ, Panagopoulos G (2010) Fragility curves for reinforced concrete buildings in Greece, *Structural and Infrastructure Engineering* 6(1-2):39-53.

Khattri KN, Rogers AM, Perkins DM, Algermissen ST (1984) A seismic hazard map of India and adjacent areas, *Tectonophysics* 108:93-134.

Khattri KN (1999) An evaluation of earthquakes hazard and risk in northern India, *Himalayan Geology* 20:1-46.

Krawinkler H, Seneviratna GDPK (1998) Pros and cons of a pushover analysis of seismic performance evaluation, *Engineering Structures* 20:452-464.

Kumar A, Anbazhagan P, Sitharam TG (2013) Seismic hazard analysis of Lucknow considering local and active seismic gaps, *Natural Hazards* 69:327-350.

Kumar A, Mittal H, Sachdeva R, Kumar A (2012) Indian strong motion instrumentation network, *Seismological Research Letters* 83:59-66.

Lang DH, Singh Y, Prasad JSR (2012) Comparing empirical and analytical estimates of earthquake loss assessment studies for the city of Dehradun, India, *Earthquake Spectra* 28:595-619.

Lang DH (2013) Earthquake damage and loss assessment–predicting the unpredictable.

Li S, Wang Q, Chen G, He P, Ding K, Chen Y, Zou R (2019) Interseismic Coupling in the Central Nepalese Himalaya: Spatial Correlation with the 2015 Mw 7.9 Gorkha Earthquake, *Pure and Applied Geophysics* 1-9.

Mahajan AK, Thakur VC, Sharma ML, Chauhan M (2010) Probabilistic seismic hazard map of NW Himalaya and its adjoining area, India, *Natural Hazards* 53:443-457.

Molina S, Lindholm C (2005) A logic tree extension of the capacity spectrum method developed to estimate seismic risk in Oslo, Norway, *Journal of Earthquake Engineering* 9:877-97.

Molina S, Lang DH, Lindholm CD (2010) SELENA–An open-source tool for seismic risk and loss assessment using a logic tree computation procedure, *Computers and Geosciences* 36(3):257-69.

Molina S, Lang DH, Meslem A, and Lindholm C (2015) SELENA v6.5-User and Technical Manual v6.5. Report no. 15-008, Kjeller (Norway) – Alicante (Spain).

McGuire RK (1976) FORTRAN computer program for seismic risk analysis (No. 76-67). US Geological Survey.

McGuire RK (2004) Seismic hazard and risk analysis, EERI Original Monograph Series MNO-10, Earthquake Engineering Research Institute, Oakland, U.S., 221 pp.

Nanda RP, Paul NK, Chanu NM, Rout S (2015) Seismic risk assessment of building stocks in Indian context, *Natural Hazards* 78:2035-51.

Nath SK, Adhikari MD, Maiti SK, Ghatak C (2019) Earthquake hazard potential of Indo-Gangetic Foredeep: its seismotectonism, hazard, and damage modeling for the cities of Patna, Lucknow, and Varanasi, *Journal of Seismology* 1-45.

Nath SK, Raj A, Thingbaijam KKS, Kumar A (2009) Ground motion synthesis and seismic scenario in Guwahati city; a stochastic approach, *Seismological Research Letters* 80:233–242.

Nath SK, Thingbaijam KKS (2012) Probabilistic seismic hazard assessment of India, *Seismological Research Letters* 83:136–149.

NDMA (2011) Development of probabilistic seismic hazard map of India, Technical Report, Working Committee of Experts (WCE), National Disaster Management Authority (NDMA), New Delhi, India.

Parvez IA, Vaccari F, Panza GF (2003) A deterministic seismic hazard map of India and adjacent areas, *Geophysics Journal International* 155:489-508.

PESMOS Department of Earthquake Engineering, Indian Institute of Technology, Roorkee.

Petersen MD, Rastogi BK, Schweig ES, Harmsen SC, Gomberg JS (2004) Sensitivity analysis of seismic hazard for the northwestern portion of the state of Gujarat, India, *Tectonophysics* 390:105-115.

Porter K, Scawthorn C (2007) Open-source risk estimation software. Technical Report, SPA Risk, Pasadena, United States of America.

Prasad JS, Singh Y, Kaynia AM, Lindholm C (2009) Socioeconomic clustering in seismic risk assessment of urban housing stock, *Earthquake spectra* 25(3):619-41.

Prasad J (2010) Seismic vulnerability and risk assessment of Indian urban housing. Ph.D Thesis, Indian Institute of Technology, Roorkee (IITR).

Raghucharan MC, Somala SN (2018) Seismic damage and loss estimation for central Indo-Gangetic Plains, India, *Natural Hazards* 94:883-904.

Raghucharan MC, Somala SN, Rodina S (2019) Seismic attenuation model using artificial neural networks, *Soil Dynamics and Earthquake Engineering* 126:105828.

Rajendran CP, Rajendran K (2005) The status of central seismic gap: a perspective based on the spatial and temporal aspects of the large Himalayan earthquakes, *Tectonophysics* 395(1-2):19-39.

Rajendran CP, John B, Rajendran K (2015) Medieval pulse of great earthquakes in the central Himalaya: Viewing past activities on the frontal thrust, *Journal of Geophysical Research: Solid Earth* 120(3):1623-41

Registrar General & Census Commissioner, India (2012) Census of India 2011

Rong Y, Pagani M, Magistrale H, Weatherill G (2017) Modeling seismic hazard by integrating historical earthquake, fault, and strain rate data. In 16th international conference on earthquake engineering.

Sharma ML, Malik S (2006) Probabilistic seismic hazard analysis and estimation of spectral strong ground motion on bed rock in north east India. In 4th international conference on earthquake engineering (pp. 12-13).

Sitharam TG, Kolathayar S (2013) Seismic hazard analysis of India using areal sources, *Journal of Asian Earth Science* 62:647–653.

The MathWorks Inc. (2017). MATLAB R2017a - academic use, the language of technical computing.

Verma M, Bansal BK (2013) Seismic hazard assessment and mitigation in India: an overview, *International Journal of Earth Sciences* 102:1203-18.

Wyss M, Gupta S, Rosset P (2017) Casualty estimates in two up-dip complementary Himalayan earthquakes, *Seismological Research Letters* 88:1508-1515.

Wyss M, Gupta S, Rosset P (2018) Casualty estimates in repeat Himalayan earthquakes in India, *Bulletin of Seismological Society of America* 108:2877-2893.

Wald DJ, Allen TI (2007) Topographic slope as a proxy for seismic site conditions and amplification, *Bulletin of Seismological Society of America* 97:1379–1395.

Xu X, Zhou X, Huang X, Xu L (2017) Wedge-failure analysis of the seismic slope using the pseudodynamic method, International Journal of Geomechanics 17(12):04017108.

Xu ZX, Zhou XP (2018) Three-dimensional reliability analysis of seismic slopes using the copula-based sampling method, Engineering Geology 242:81-91.

Zhou XP, Cheng H (2014) Stability analysis of three-dimensional seismic landslides using the rigorous limit equilibrium method, Engineering geology 174:87-102.

Zhou X, Qian Q, Cheng H, Zhang H (2015) Stability analysis of two-dimensional landslides subjected to seismic loads, Acta Mechanica Solida Sinica 28(3):262-76.

Zhou X, Cheng H, Wong LN (2019) Three-dimensional stability analysis of seismically induced landslides using the displacement-based rigorous limit equilibrium method, *Bulletin of Engineering Geology and the Environment* 78(7):4743-56.